Electric and Electrophoretic Inversion of the DNA Charge in Multivalent Electrolytes

Binquan Luan[*] and **Aleksei Aksimentiev**[†]

[*]IBM Physical Science Division, PO Box 218, Yorktown Heights, New York 10598

[†]Department of Physics, University of Illinois at Urbana-Champaign, 1110 W. Green Street, Urbana, Illinois 61801, USA aksiment@illinois.edu

Abstract

Counterion-induced inversion of the DNA charge was characterized through extensive molecular dynamics simulations. We observed reversal of the DNA motion in an external electric field upon increasing the concentration of trivalent or quadrivalent counterions. In the case of a divalent electrolyte, inversion of the DNA's electric charge was observed at high concentrations of the electrolyte but not reversal of the DNA' electrophoretic motion. We demonstrate that inversion of the DNA's electrophoretic mobility results from a complex interplay of electrostatics and hydrodynamics.

As a highly charged polymer, DNA exhibits unusual electrostatic properties that are thought to play a role in the fundamental biological process – packaging DNA into compact structures. Thus, depending on the properties of the surrounding electrolyte, the character of interaction between two identical DNA molecules can change from repulsion to attraction.[1] In a high-concentration multivalent electrolyte, the theory of counterion correlation[2] predicts an inversion of the DNA's electric charge, which might be manifested as a reversal of the DNA's motion in an external electric field. The latter phenomenon was only recently demonstrated in experiment.[3] While counterion condensation reduces or even inverts the DNA charge, the counterions may still be mobile at the DNA surface. Subject to an external electric field, the mobile counterions can produce an electro-osmotic flow[4] and exert a hydrodynamic drag on DNA.[5] This hydrodynamic effect obscures the relation between inversion of the DNA's electric charge and reversal of the DNA's electrophoretic mobility. Ideally, the mechanism of the charge inversion (CI) would be elucidated by a simultaneous measurement of the DNA's electrophoretic mobility and the distribution of counterions around DNA. As such measurements remain extremely difficult, in this work, we report molecular dynamics (MD) simulations that elucidate complex interplay of electrostatics and hydrodynamics in determining the conditions for the reversal of the DNA's electrophoretic motion and clarify the relationship of the latter to the inversion of the DNA's electric charge.

Figure 1(a) illustrates the simulation system. A poly(dA)·poly(dT) fragment of dsDNA (one helical turn in length) was submerged in electrolyte and confined to a wide, 30-Å-radius nanochannel that provided a well-defined no-slip boundary condition to the flow of electrolyte and served as a heat sink. We chose this setup to avoid uncontrolled finite-size artifacts of free-solution simulations, for example, an artificial viscous force produces by the thermostat. Furthermore, electric field-driven transport of DNA through a nanochannel is a problem of considerable scientific and technological interest.[6] A periodic boundary condition was imposed in all three directions. The 5' and 3' ends of each DNA stand were covalently linked over the periodic boundary of the system. The electrolyte consisted of water molecules, *spermine*[4+] (*spm*[4+]), *spermidine*[3+] (*spd*[3+]), Mg^{2+} or Na^+ counterions, and chloride coions added to

neutralize the systems. The nanochannel was cut from a Si_3N_4 crystal; the nanochannel surface had the total electric charge of 0.[7] Each simulation system contained about 31,000 atoms.

Following assembly, each system was minimized and equilibrated in the NVT ensemble for 50 ps using the program NAMD,[8] charmm force field for DNA,[9] custom force field for Si_3N_4,[7] TIPS3P model of water,[10] particle-mesh Ewald (PME) electrostatics and multiple time stepping.[11] Van der Waals interactions were calculated using a smooth (10–12 Å) cutoff. The temperature was kept constant by applying a Langevin thermostat[12] with a damping rate 0.1 ps^{-1} to atoms of the nanochannel. Subsequently, each system was simulated for tens of nanoseconds in a uniform electric field of $E_0 = 78$ mV/nm directed parallel to the DNA axis. We have previously shown[5] that the electrophoretic force linearly increases with the electric field strength for E_0 values of that order. Furthermore, because the electric field was applied along the helical axis of DNA, the radial distribution of counterions was similar to that in the absence of the field. Using this setup we could investigate the relationship between the inversion of the DNA's electric charge and the reversal of the DNA's electrophoretic mobility in the same simulation. In all simulations, DNA was constrained to the center of the nanochannel by a radial harmonic restraint that applied to the center of mass of the phosphorus atoms; DNA was free to move along the axis of the nanochannel. Such a constrain did not distort the canonical conformation of DNA. Another set of harmonic restraints was applied to the nanochannel, constraining its position. The third set of constraints applied to all ions to prevent their adhesion to the nanochannel surface. [5] We show in Supplementary Data that the last set of constrains is equivalent to coating the surface with a layer of amine groups.

The electrophoretic motion of DNA in spm^{4+} electrolyte is characterized in Fig. 1b. After first ~10 ns, DNA was observed to move quasi-steadily, indicating a balance between the force of the external electric field and the hydrodynamic friction. The three simulated systems contained 5, 10 and 20 spm^{4+} ions, corresponding to 0, 0.1 and 0.3 M spm^{4+} concentrations. Note, that we compute the electrolyte concentration based on the number of counterions in excess to the number required to compensate the charge of the DNA fragment $-20e$, where e is one proton charge. In the zero concentration limit, DNA moves opposite the electric field direction. At 0.3 M, DNA'e electrophoretic motion is in the direction of the external electric field, indicating a possible CI. At 0.1 M, DNA moves both along and against the electric field, alternating direction every several nanoseconds; the overall motion is in the field direction.

In Fig. 2, we plot the electrophoretic mobility of DNA μ versus the concentration of spm^{4+}, spd^{3+}, Mg^{2+} and Na^+ electrolytes, defining $\mu = v/E_0$, where v is the velocity of DNA and E_0 is the electric field. As the concentration of spm^{4+} or spd^{3+} increases, the DNA's mobility changes from a negative to a positive value, in agreement with experiment.[3] For Na^+ and Mg^{2+} electrolytes, increasing the counterion concentration was observed to reduce the DNA's mobility without changing its sign.

The observed reversal of the DNA's electrophoretic motion in spm^{4+} and spd^{3+} electrolytes could be related to the high affinity of spm^{4+} and spd^{3+} counterions to DNA. Figure 3a illustrates a typical conformation observed in our simulations, where two spm^{4+} ions are bound to the minor groove of DNA. Although these counterions remain bound to the minor groove for the entire duration of our simulations, they are mobile and can move along the minor groove. [13] For Na^+ or Mg^{2+} counterions, no specific binding to DNA was observed. The residence time of these counterions at the DNA surface was found to be, in our simulations, about 10 pS, which is consistent with the small-angle x-ray scattering data showing that divalent counterions are not absorbed at the surface of DNA, but are distributed as a compact cloud around it.[14] Subject to an external electric field, the counterion cloud can be displaced along the DNA surface, producing an electroosmotic flow.[5]

To characterize the distribution of the electric charge around DNA, we defined a cumulative charge density $q(R)=(\Sigma_{r_i<R} Q_i)/V(r < R)$, where Q_i is the charge of ith atom (DNA or ion) inside a cylinder of radius R and V is the volume of the cylinder. Figure 3(b) shows $q(R)$ averaged over the last 20 ns of each simulation. For comparison, the inset to Fig. 3b shows $q(R)$ for the DNA fragment only. Due to the charged phosphate groups, $q(R)$ is most negative at $R \sim 12$ Å. In all spm^{4+} systems, two spm^{4+} molecules were found in the minor groove of the DNA fragment (Fig. 3(a)). Therefore, $q(R < 15$ Å$)$ for DNA in spm^{4+} electrolyte is less negative than for bare DNA. As the concentration of spm^{4+} increases, more spm^{4+} are found in the major groove. For the DNA sequence used in our simulations, spm^{4+} are more mobile in the major groove than in the minor groove. When this DNA fragment is solvated, water molecules bridge the N3 and O2 atoms of neighboring base pairs, forming a "water-spine" in the minor grove. As a spm^{4+} molecule contains many hydrogen donors, the "water spine" can be replaced by spm^{4+} counterions. For other DNA sequences, spm^{4+} was found to have high affinity to the major groove as well.[15]

In the zero concentration limit of the spm^{4+} electrolyte, $q(R)$ is always negative away from the DNA surface ($R >12$Å). At 0.1 and 0.3 M spm^{4+} concentrations, $q(R)$ becomes positive at 17 Å and 15 Å, respectively, indicating inversion of the DNA's electric charge due to overscreening by spm^{4+} counterions. The presence of a nanochannel in our simulations does not contribute to the overscreening effect, as the nanochannel radius is much greater than the Debye screening length of the solution. Thus, we observed the electric CI to occur several angstroms away from the DNA surface, not at the DNA surface, which can be due to the electrostatic repulsion of the counterions. The spm^{4+} counterions were observed to attach with one end to the DNA surface, for example, a phosphate group, whereas the other end reached out into the electrolyte. In an external electric field, the connection between spm^{4+} and DNA could frequently break and reform. Nevertheless, our observations are in accord with the idea of fractionalization of the polymer counterion charge used in theoretical models of DNA CI. [16] Here, we emphasize that the inversion of the DNA's electric charge is determined by the radial distribution of the counterions.

In an electric field, spm^{4+} near the DNA surface are mobile and could move in the field direction, producing an electroosmotic flow. Mediated by the flow, only a fraction of spm^{4+} momentum transfers to DNA while the rest is absorbed by the nanopore surface. It is commonly thought that reversal of the electrophoretic motion indicates inversion of the DNA's electric charge. However, complicated by the hydrodynamic shearing, reversal of the electrophoretic motion only indicates inversion of the DNA's effective charge $\xi \mu$,[5] where ξ is the friction coefficient and μ is the electrophoretic mobility. Hence, when DNA changes the direction of its motion, its electrophoretic mobility μ changes its sign. Consequently, the effective charge of DNA changes its sign.

To illustrate the hydrodynamic effect, we computed the velocity profile of the water flow, Fig. 3(c). Near the DNA surface, water moves approximately with the same velocity as the DNA fragment; the water velocity is zero near the nanochannel surface. In the zero-limit concentration, water between the DNA and the nanochannel moves in the direction of the DNA's motion, opposite the electric field. At a 0.1 M concentration, the water flow has a maximum around 15 Å. In that region, spm^{4+} moves faster in the direction of the electric field than the DNA. Driven by the motion of spm^{4+}, water moves faster than the DNA as well, exerting a shear force on the DNA. At higher spm^{4+} concentrations, water flow attains a maximum at the DNA surface. As a consequence of the electric CI shown in Fig. 3(b), chloride ions behave like counterions of the DNA-spm^{4+} complex and occupy the region near the nanochannel surface. Therefore, in an external electric field, water near the nanopore surface moves opposite the field direction, driven by the motion of chloride ions (Fig. 3(c)). That is, the direction of the electro-osmotic flow changes its sign away from the DNA surface.

In the above discussion we defined two types of CI: electric and electrophoretic. The former is conditioned by the radial distribution of counterions around DNA, whereas the latter depends on both electrostatic and hydrodynamic effects. In our setup, the electro-osmotic flow transmits only a fraction of the electrostatic force on the counterions to DNA whereas the remaining fraction of that force is balanced by the friction with the nanochannel. Therefore, only a fraction of a counterion's charge contributes to the DNA's electrophoretic charge, while the whole charge of the same counterion contributes to the radial screening of the electric charge. It is likely that, at some intermediate counterion concentration, inversion of the electric charge (i.e. $q(R) > 0$) does take place whereas reversal of the electrophoretic motion does not (see below). Hence, reversal of the DNA's electrophoretic motion is sufficient to indicate electric CI.

Figure 4 shows the cumulative charge density and the water velocity profiles in the simulations of the spd^{3+}, Mg^{2+} and Na^+ electrolyte systems. In the case of the spd^{3+} electrolyte (Fig. 4(a) (b)), the simulation results are very similar to those obtained in the spm^{4+} case. Increasing the spd^{3+} concentration reverses direction of the DNA's electrophoretic motion, which can be discerned from the water flow profiles (Fig. 4(a)) in the limit of small R. At 0.14 M, the water velocity profile has a maximum at $R = 15$ Å, which is indicative of the hydrodynamic drag on the DNA by the electro-osmotic flow. The cumulative charge density $q(R)$ becomes positive around 17 Å in the 0.42 M spd^{3+} system, Fig. 4(b), indicating an electric CI. In these simulations, three spd^{3+} ions were observed to enter the minor groove of DNA and align head-to-tail.

In Mg^{2+} or Na^+ electrolytes, DNA was always observed to move opposite the electric field direction despite the high ion concentrations (Fig.4(c)(e)). Due to considerable reduction of the DNA's electrophoretic mobility, long (over 80 ns) simulation trajectories were required to conclude about the character of the DNA motion. In Mg^{2+} electrolytes, the electro-osmotic effects are evident in the water velocity profiles that peak around $R = 14$ Å (Fig. 4(c)), indicating a hydrodynamic drag force on DNA. Although this hydrodynamics force is not strong enough to change the direction of the DNA motion, the radial distribution of the cumulative charge already indicates electric CI at $R = 14$ Å (Fig. 4(d)). This directly supports our previous conclusion that the electric CI can occur before the electrophoretic one. Note that the possibility of electric CI of DNA in Mg^{2+} electrolytes was inferred from experimental studies of DNA ejection from viral capsids[17] but was not observed in the electrophoretic measurements. [3] In Na^+ electrolytes, neither electrophoretic nor electric CI were observed in our simulations (Fig. 4(e)(f)).

In conclusion, through extensive MD simulations we characterized the screening of the electric charge and the electrophoretic mobility of DNA in multivalent electrolytes. In trivalent or quadrivalent electrolytes, DNA was found to reverse direction of its electrophoretic motion upon increasing the concentration of counerions beyond a threshold value. This, strictly speaking, indicates the inversion of the DNA's effective charge ($\xi\mu$). The inversion of the DNA's electric charge could occur at a counterion concentration below the threshold. In divalent electrolytes, only electric CI was observed. Experimentally, reversal of the DNA's electrophoretic mobility was found to occur at ion concentrations much lower than those examined in our MD simulations. The finite size of the simulation systems and discrete nature of the counterion charge impede detailed characterization of the millimolar concentration range. We expect, however, the physical insights gained through simulations of higher concentration systems to be directly applicable to the low concentration regime. From a practical point, our study demonstrates the possibility of controlling the DNA motion in a nanochannel by varying the concentration and composition of the electrolyte, which may find applications in bionanotechnology.

Supplementary Material

Refer to Web version on PubMed Central for supplementary material.

Acknowledgments

References

1. Bloomfield V. Biopolymers 1997;44:269–282. [PubMed: 9591479] Nguyen T, Rouzina I, Shklovskii B. J. Chem. Phys 2000;112:2562.Luan B, Aksimentiev A. J. Am. Chem. Soc 2008;130:15754–15755. [PubMed: 18975864] Baldwin GS, Brooks NJ, Robson RE, Wynveen A, Goldar A, Leikin S, Seddon JM, Kornyshev AA. J. Phys. Chem. B 2008;112:1060–1064. [PubMed: 18181611]

2. Shklovskii B. Phys. Rev. E 1999;60:5802.Grosberg A, Nguyen T, Shklovskii B. Rev. Mod. Phys 2002;74:329–345.

3. Besteman K, Van Eijk K, Lemay S. Nature Phys 2007;3:641.

4. Nkodo AE, Garnier JM, Tinland B, Ren H, Desruissaux C, Mc-Cormick LC, Drouin G, Slater GW. Electrophoresis 2001;22:2424. [PubMed: 11519946]

5. Luan BQ, Aksimentiev A. Phys. Rev. E 2008;78:021912.Long D, Viovy JL, Ajdari A. Phys. Rev. Lett 1996;76:3858. [PubMed: 10061127] Ghosal S. Phys. Rev. E 2007;76:061916.van Dorp S, Keyser U, Dekker N, Dekker C, Lemay S. Nature Phys 2009:347–351.

6. Branton D, Deamer D, Marziali A, Bayley H, Benner S, Butler T, Di Ventra M, Garaj S, Hibbs A, Huang X, et al. Nature Biotech 2008;26:1146–1153.

7. Aksimentiev A, Heng JB, Timp G, Schulten K. Biophys. J 2004;87:2086–2097. [PubMed: 15345583]

8. Phillips JC, et al. J. Comp. Chem 2005;26:1781. [PubMed: 16222654]

9. MacKerell AD Jr, Banavali NK. J. Comp. Chem 2000;21:105–120.

10. Jorgensen WL, Chandrasekhar J, Madura JD, Impey RW, Klein ML. J. Chem. Phys 1983;79:926–935.

11. Batcho PF, Case DA, Schlick T. J. Chem. Phys 2001;115:4003–4018.

12. Allen, MP.; Tildesley, DJ. Computer Simulation of Liquids. New York: Oxford University Press; 1987.

13. Korolev N, Lyubartsev A, Laaksonen A, Nordenskiold L. Biophys. J 2002;82:2860–2875. [PubMed: 12023210]

14. Morfin I, Horkay F, Basser P, Bley F, Hecht A, Rochas C, Geissler E. Biophys. J 2004;87:2897–2904. [PubMed: 15454479]

15. Feuerstein B, Pattabiraman N, Marton L. Proc. Natl. Acad. Sci. USA 1986;83:5948–5952. [PubMed: 3461466] Feuerstein B, Pattabiraman N, Marton L. Nucl. Acids Res 1990;18:1271. [PubMed: 2320418]

16. Nguyen T, Shklovskii B. Phys. Rev. Lett 2002;89:1.

17. Evilevitch A, Fang L, Yoffe A, Castelnovo M, Rau D, Parsegian V, Gelbart W, Knobler C. Biophys. J 2008;94:1110–1120. [PubMed: 17890396] Lee S, Tran CV, Nguyen TT. arXiv:0811.1296 [cond-mat.soft]. 2008
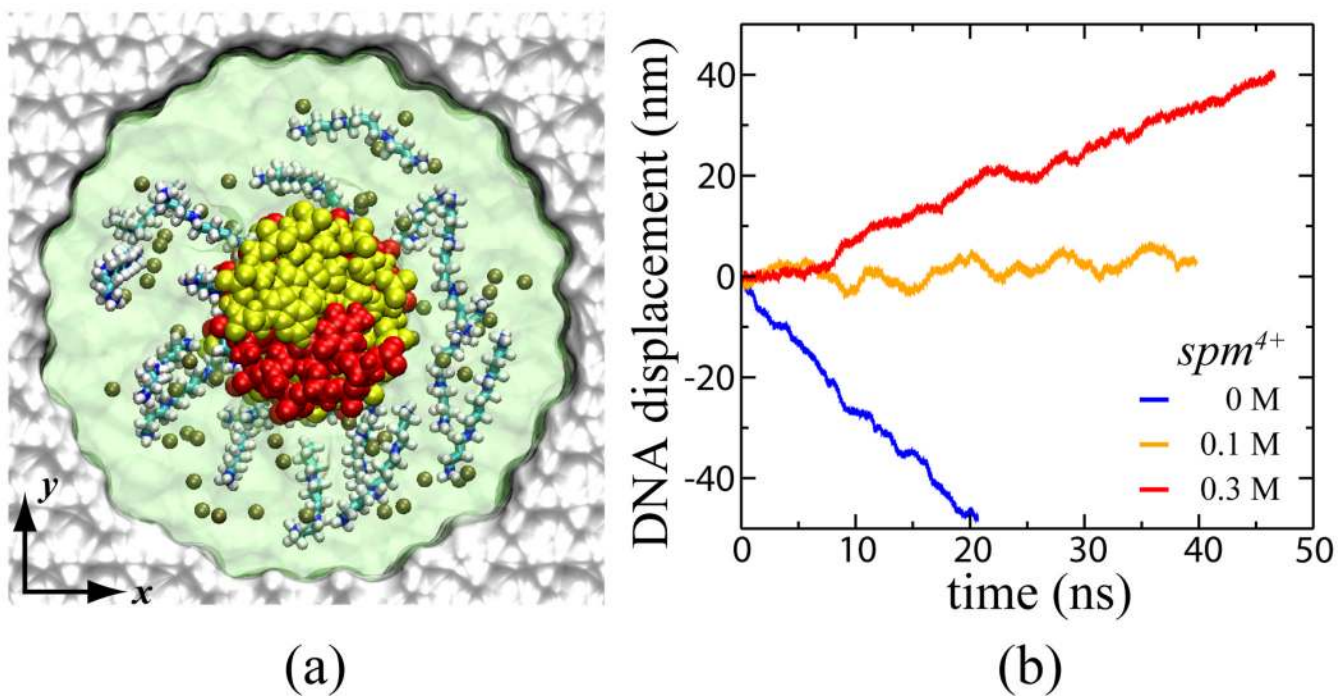
Figure 1.
(a) Setup of MD simulations. Two strands of a DNA helix are shown in yellow and red; spm^{4+} ions as balls and sticks; chloride (tan) ions as vdW spheres; water and nanochannel as transparent and solid-color (white) surfaces, respectively. (b) Simulated displacement of DNA. The concentration of 0, 0.1 and 0.3 M corresponds to 5, 10 and 20 spm^{4+} ions in the simulation systems (see text).
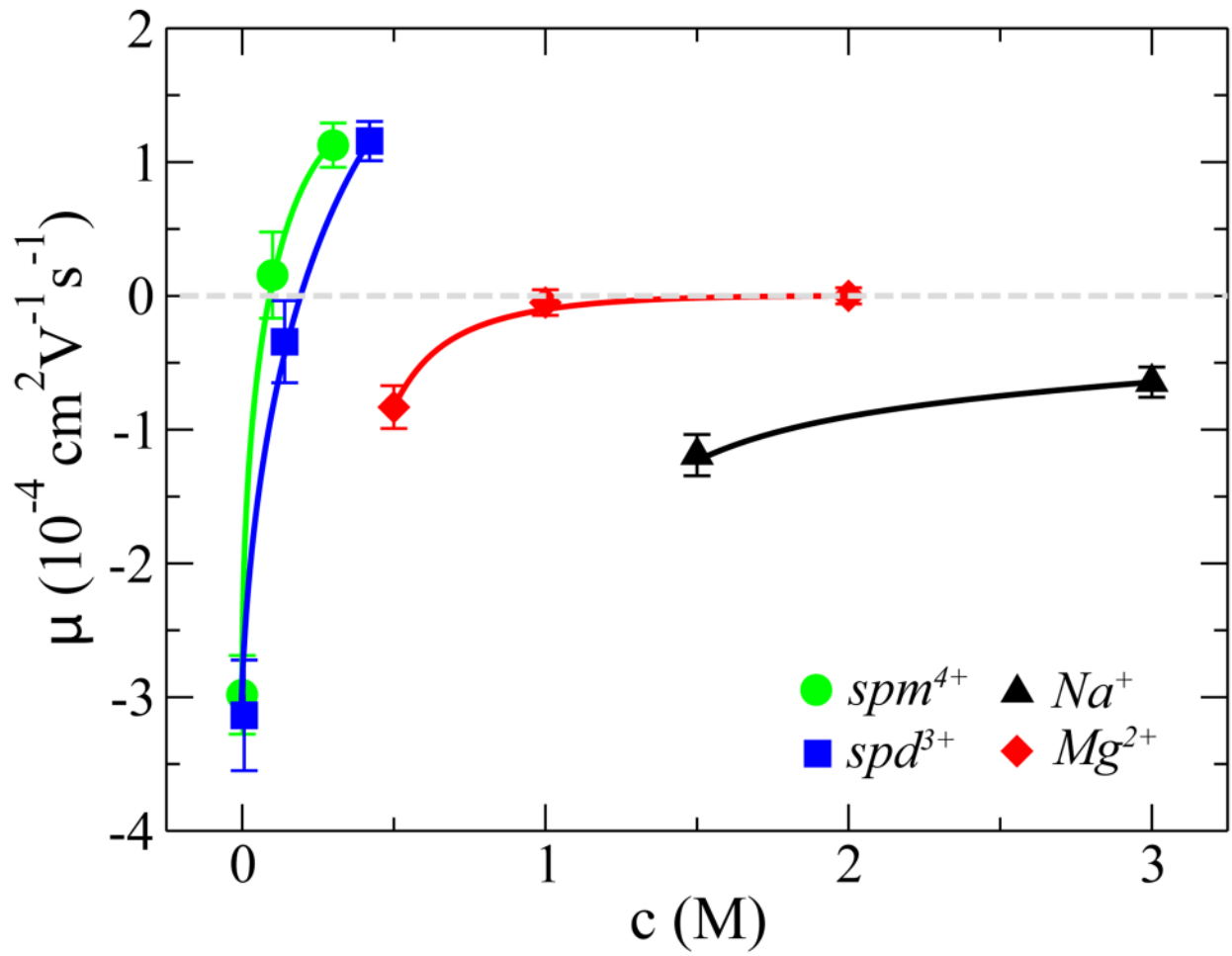
Figure 2.
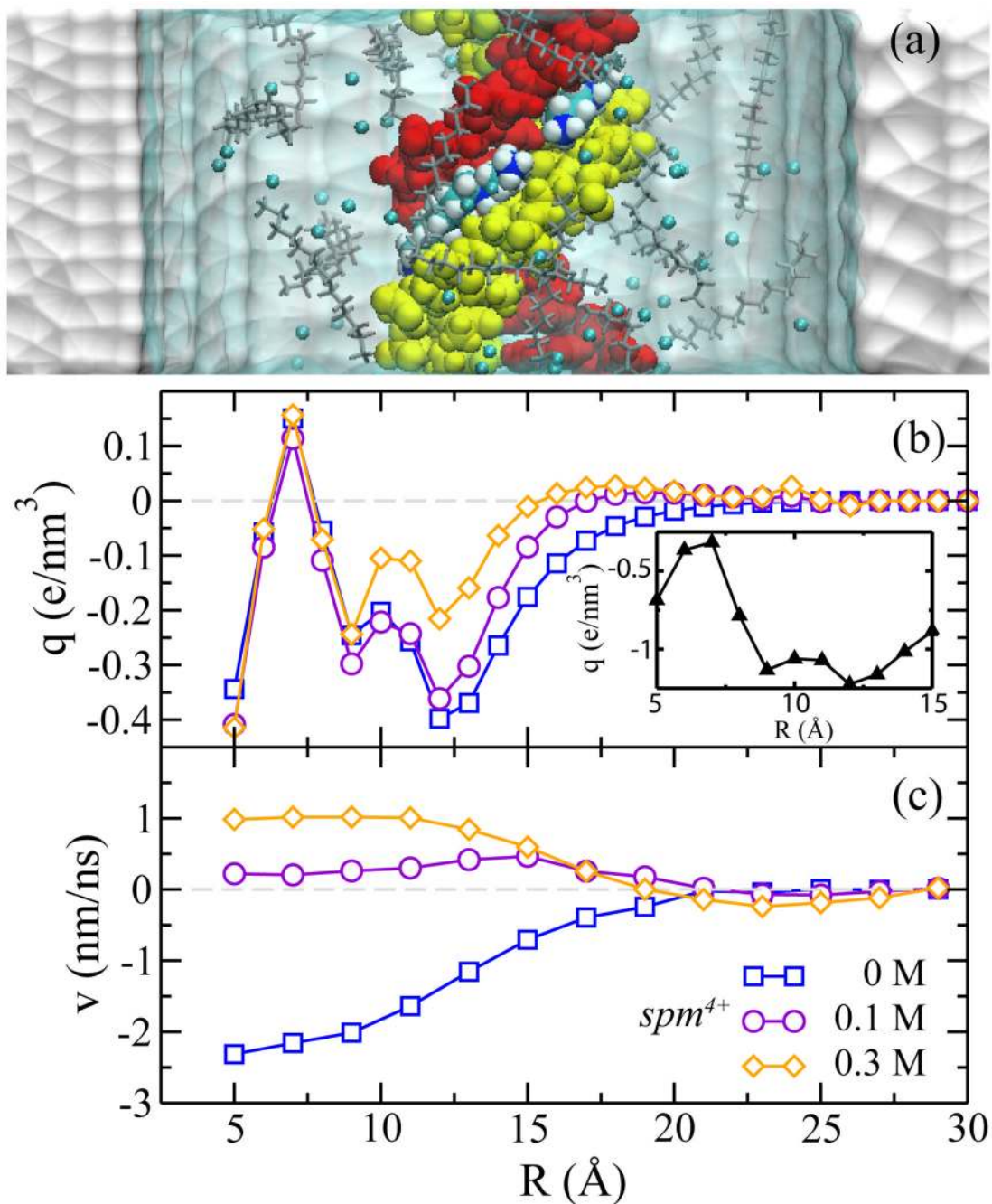Electrophoretic mobility of DNA versus counterion concentration. Lines are guides to the eye.

Figure 3.
Charge inversion in *spm*[4+] electrolyte. (a) Side-view of the simulation system. In this
simulation, the DNA moves in the direction of the electric field. Two *spm*[4+] ions in the minor
groove of the DNA are shown as van der Waals spheres; all other *spm*[4+] ions are shown in the
stick representation. (b) Cumulative charge density versus distance from the DNA's center.
Inset: Cumulative charge density of the bare DNA. (c) Velocity of the water flow versus
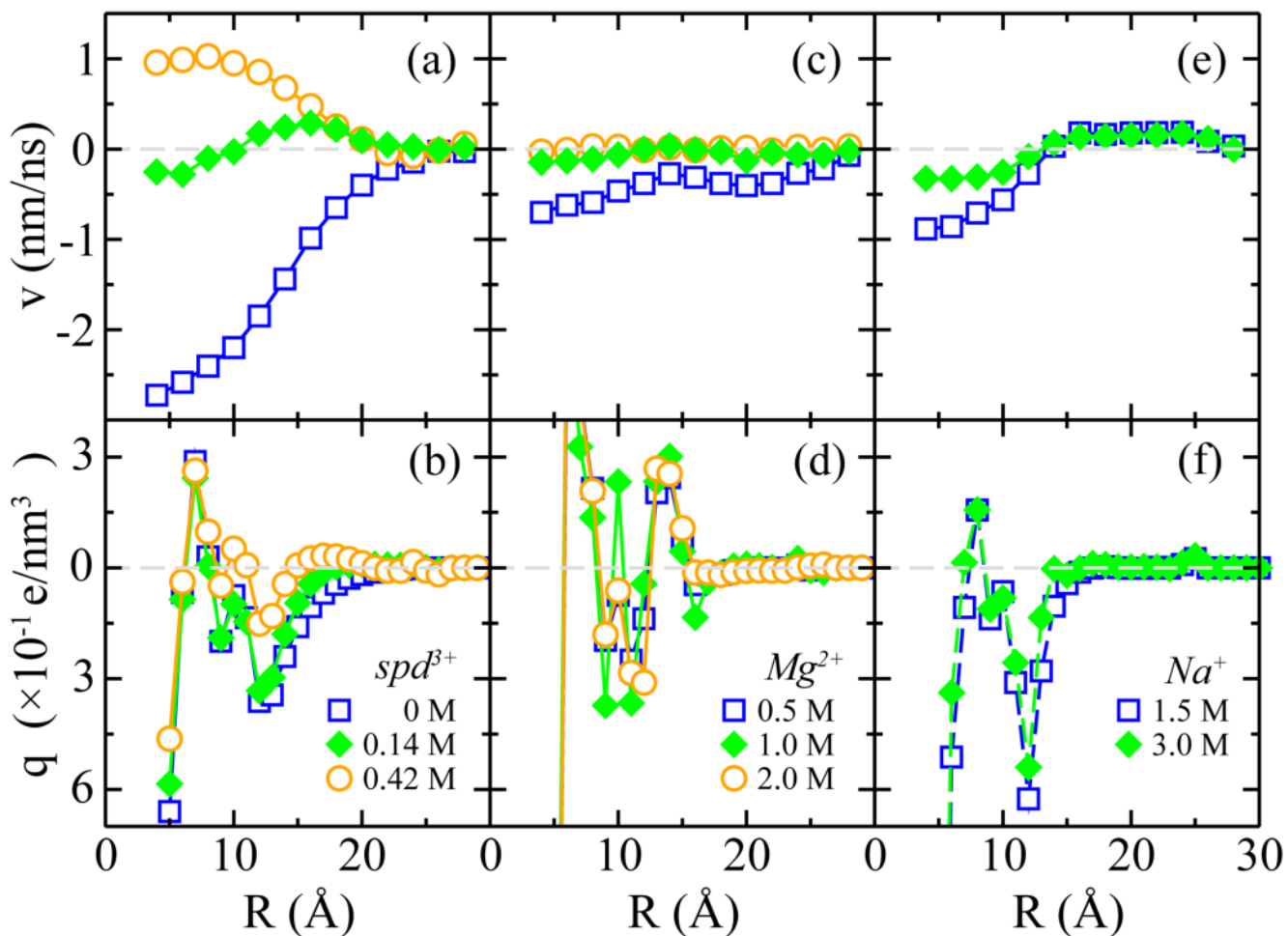distance from the DNA's center.

Figure 4.
Effective and electric CI in spd^{3+}, Mg^{2+} or Na^+ electrolytes. (a,c,e) Velocity of the water flow in the simulated systems measured from the DNA's center. (b,d,f) Cumulative charge density versus distance from the DNA's center.